Published in final edited form as:
Cell Mol Bioeng. 2009 June 1; 2(2): 231–243. doi:10.1007/s12195-009-0060-z.

Cell Structure Controls Endothelial Cell Migration under Fluid Shear Stress

Xiefan Lin[1] and **Brian P. Helmke**[1,2]

[1]Department of Biomedical Engineering, University of Virginia, P. O. Box 800759, Charlottesville, Virginia 22908

[2]Robert M. Berne Cardiovascular Research Center, University of Virginia, P. O. Box 800759, Charlottesville, Virginia 22908

Abstract

Cobblestone-shaped endothelial cells in confluent monolayers undergo triphasic mechanotaxis in response to steady unidirectional shear stress, but cells that are elongated and aligned on micropatterned substrates do not change their migration behavior in response to either perpendicular or parallel flow. Whether mechanotaxis of micropatterned endothelial cell layers is suppressed by elongated cytoskeletal structure or limited availability of adhesion area remains unknown. In this study, cells were examined on wide (100–200 μm) micropatterned lines after onset of shear stress. Cells in center regions of the lines exhibited cobblestone morphology and triphasic mechanotaxis behavior similar to that in unpatterned monolayers, whereas cells along the edges migrated parallel to the line axis regardless of the flow direction. When scratch wounds were created perpendicular to the micropatterned lines, the cells became less elongated before migrating into the denuded area. In sparsely populated lines oriented perpendicular to the flow direction, elongated cells along the upstream edge migrated parallel to the edge for 7 h before migrating parallel to the shear stress direction, even though adhesion area existed in the downstream direction. Thus, cytoskeletal structure and not available adhesion area serves as the dominant factor in determining whether endothelial mechanotaxis occurs in response to shear stress.

KEY TERMS

cell motility; shear stress; mechanotransduction; mechanotaxis; micropatterning

INTRODUCTION

Spatially varying arterial hemodynamic shear stress profiles in vivo have been implicated in the focal development of atherosclerotic lesions,[6, 7, 14] primarily through control of endothelial cell (EC) gene expression and function. In athero-resistant regions of the vessel wall where unidirectional laminar shear flow exists, ECs are elongated in shape and aligned with the direction of flow. Near bifurcations and curved regions where the flow profile is "disturbed" and atherogenesis is more likely, ECs take a more polygonal shape.[6, 27, 36] An inflamed endothelial phenotype develops, which serves to increase macromolecule barrier permeability and to recruit immune cells. Similar phenotype adaptations are induced by shear stress profiles in vitro. For example, cultured ECs adapt their shape and cytoskeletal

Address for correspondence: Brian P. Helmke, Ph.D., Department of Biomedical Engineering, University of Virginia, P. O. Box 800759, Charlottesville, VA 22908, Tel. +1 434-924-1726, Fax +1 434-982-3870, helmke@virginia.edu.

structure from polygonal to elongated and aligned after exposure to unidirectional laminar shear flow for approx. 24 h.[9, 22]

Local mechanical forces such as shear stress profile also regulate the EC migration, which plays a critical role in the processes of angiogenesis,[21] wound healing,[5] and stent re-endothelialization.[32] In vitro, isolated ECs in a subconfluent layer extend lamellipodia in the direction of shear stress within minutes after onset.[4, 24] Within 30 min, they migrate in the downstream direction in a process referred to as “mechanotaxis”.[24] In scratch-wounded confluent EC monolayers, migration speed into the wound area is increased in cells migrating from the upstream wound edge in the direction of flow compared to that in cells migrating from the downstream wound edge.[18] ECs within confluent monolayers undergo a triphasic response, initially migrating in the upstream direction after flow onset followed by downstream-directed migration on an adaptation time scale.[25] In confluent layers, the development of increased motility and directional persistence after preconditioning to an arterial shear stress waveform requires the presence of serum growth factors and involves Par6-dependent junctional complexes associated with planar cell polarity.[31]

Planar cell polarity and cell shape exert a strong influence over cell motility characteristics even in the absence of shear stress. For example, isolated cells grown on 15-μm strips fabricated by micropatterning exhibited an elongated morphology and migrated faster than single cells on wider strips or on unpatterned surfaces.[23] One hypothesis to explain increased motility involves the idea that directional prestress associated with cytoskeletal structure in elongated cells contributes to directional lamellipodium extension and polarity. Indeed, ECs grown on micropatterned square islands exhibited stress fibers that were oriented diagonally, and lamellipodia were extended preferentially from the corners.[3] In contrast, ECs on round islands extended lamellipodia in random directions. Furthermore, when asymmetrically shaped cells were allowed to migrate off teardrop-shaped islands after release of the micropatterned shape restriction, they preferentially extended lamellipodia out from the blunt end and then migrated in that direction.[20] Thus, pre-existing cell structure must contribute to directional cell motility.

Although both cell structure and motility adapt to the local mechanical environment, it remains unknown whether these two adaptation processes are mutually independent or whether pre-existing cell structure desensitizes EC mechanotaxis in response to hemodynamic forces. One method to examine this question is to preset EC structure using micropatterned lines of extracellular matrix protein before exposure to shear stress.[19, 25, 37] Shear stress–dependent mechanotaxis is reduced in elongated ECs on 20-μm wide lines of fibronectin;[25] however, it is possible that mechanotaxis could not occur simply because geometric patterning did not provide available adhesion area in the downstream direction. In order to test the hypothesis that EC shape and cytoskeletal structure and not adhesion area was responsible for reduced mechanotaxis of elongated ECs, the present studies examined EC migration as a function of cell shape on wider micropatterned lines during exposure to steady unidirectional shear stress (Figure 1). If the hypothesis is true, then one would predict that polygonal-shaped cells located in the center of the wide lines would behave similarly to ECs in a confluent monolayer (Figure 1A), whereas elongated ECs at the edges of the lines (Figure 1B) would behave similarly to ECs on narrow micropatterned lines. Furthermore, on micropatterns that have adhesion area available in the downstream direction (Figure 1C–D), ECs would be predicted to immediately undergo mechanotaxis if cell shape and structure were not critical factors. The results of these studies demonstrate that elongated cell shape and cytoskeletal structure serves to desensitize EC mechanotaxis in response to shear stress.

MATERIALS AND METHODS

Microcontact Printing

Microcontact printing was used to create fibronectin-patterned surfaces as described previously.[25] Briefly, silicon masters were fabricated by traditional photolithography techniques, and reverse patterns were transferred to poly(dimethylsiloxane) (PDMS) stamps (Sylgard 184, Dow Corning, Midland, MI). The PDMS stamps were used to transfer 2 mM 1-octadecanethiol (Aldrich, St. Louis, MO) onto Au-coated glass coverslips. After blocking with 2 mM tri(ethylene glycol)-terminated alkanethiol (ProChimia Surfaces, Poland) for 4 h, the coverslips were incubated in 30 $\mu g\ ml^{-1}$ fibronectin solution for 2 h.

Cell Culture

Primary bovine aortic ECs, passages 11–17, were cultured in a humidified 5% CO_2 incubator at 37 °C. Complete growth medium consisted of Dulbecco's Modified Eagle Medium (DMEM, Gibco, Gaithersburg, MD) supplemented with 10% heat-inactivated newborn calf serum (HyClone, Logan, UT), 2.92 mg ml^{-1} of L-glutamine (Gibco), and 1000 u ml^{-1} penicillin-streptomycin (Gibco).

Flow Experiment and Wound Healing Assay

The migration of ECs under shear stress was studied in a parallel-plate flow chamber (FCS-2, Bioptechs, Butler, PA) as described previously.[17, 25] Complete growth medium was recirculated by a peristaltic pump (Cole-Palmer Instrument Company) into an upstream reservoir and was driven by gravity into the flow chamber to create a wall shear stress of 1.5 Pa. The pH of the bicarbonate-containing perfusion medium was maintained by equilibration with humidified CO_2, and the temperature of the coverslip was maintained at 37 °C using a temperature controller (Bioptechs).

In the wound healing experiments, a surgical needle tip was used to create scratches perpendicular to the micropatterned lines just before assembly of the coverslip into the flow chamber.

Image Acquisition and Data Analysis

Time-lapse images were acquired every 5 min in bright field or phase contrast mode using a DeltaVision RT microscope system (Applied Precision, Issaquah, WA). Image frames were spatially normalized for stage drift using fluorescent microspheres (Molecular Probes, Carlsbad, CA) coated onto the coverslips as fiducial markers. Images were acquired using softWoRx software (Applied Precision) and exported into ImageJ[1] or Matlab (MathWorks, Natick, MA) for analysis.

For cell shape and migration analysis, boundaries and geometric center positions were obtained either manually or using a semi-automated algorithm described previously.[25] Cell morphology was quantified using shape index and fraction of aligned cells. Shape index was computed as $(4\pi)(Area)(Perimeter)^{-2}$. The fraction of aligned cells was defined as the proportion of cells with major axis within 20° of the micropatterned line direction. Migration directions were determined relative to the positive x-axis using the initial and final geometric centroid positions of each cell during a given time interval.

T-test or analysis of variance (ANOVA) was used for non-circular data to test the null hypothesis that means among groups were equal at a significance level of 0.05. Where required, Fisher's Least Squared Difference was used post hoc to determine individual groups that were significantly different. Migration angles were analyzed using a nonparametric circular statistics approach as described previously.[12, 25] In some

experiments, cell migration directions were categorized as left, right, and vertical, and fractions of cells migrating in each direction were computed, In these cases, proportions of cells migrating in directional categories were compared to expected values using the normal approximation of the binomial distribution. The standard error of the proportion was estimated as

$$SE_p = \sqrt{\frac{p(1-p)}{N}}$$

where p is the proportion of cells in the category of interest, and N is the total number of cells in all categories.

RESULTS

Shear-Stress–Induced Migration of ECs in Confluent Layers When Cell Shape Is Polygonal

Since ECs cultured on wide micropatterned lines of fibronectin exhibit a range of cell shapes and motility characteristics,[23] we hypothesized that this technique would serve as a tool to examine the mechanotaxis response of ECs exhibiting a range of cell shapes on a single substrate. ECs that were located in the center regions of 100–200 μm wide micropatterned lines exhibited polygonal morphology, similar to ECs in unpatterned confluent monolayers (Figure 2A). In contrast, ECs located at the edges of the micropatterns were elongated parallel to the edges. To categorize the migratory behavior of cells, lines were divided into zones: the “edge” zone consisted of the outer most 20-μm region; the next 20-μm region away from the edge was termed the “middle” zone; and the remaining central region of the pattern was defined as the “center” zone. The shape index of ECs in the center zone was 0.57±0.02 (mean±SE). This value was significantly greater than that of ECs in the edge zones, which had shape index 0.37±0.03 (Figure 2B). The fraction of aligned cells was significantly greater in the edge zones than in the center and middle zones (Figure 2C). Thus, ECs on wide micropatterned lines exhibited shape elongation and alignment that were a function of distance from the pattern edge.

If the sensitivity of EC mechanotaxis is a function of cell shape, then ECs in the center zones of wide micropatterned lines should mimic those in unpatterned confluent monolayers, but ECs in the edge zones should behave similarly to those on narrow micropatterned lines. In order to test the first part of this hypothesis, cell migration direction in response to onset of shear stress was analyzed in unpatterned confluent EC monolayers and in ECs with polygonal shape located in the center zones of wide micropatterned lines (Figure 1A). The direction of cell migration was classified as left-, right-, and vertically migrating by dividing the unit circle into sectors as illustrated in Figure 3A. In the case when cells migrate in random directions, the expected value of the fraction of right-migrating cells is 0.25, of left-migrating cells is 0.25, and of vertically migrating cells is 0.5. Consistent with this model, ECs in an unpatterned confluent monolayer exhibited constitutive migration in random directions before onset of shear stress (Figure 3B, $t < 0$ h). The fractions of left-migrating (blue) and right-migrating (red) ECs fluctuated near 0.25 (gray band indicates the 95% confidence interval of the expected value, with an average of 5370 cells tracked per 20-min interval). In addition, the fraction of vertically migrating ECs during the 4-h interval before onset of shear stress was 0.5 (light green band indicates 95% confidence interval of the expected value). In the first 4 h after onset of steady unidirectional shear stress oriented from left to right (Figure 3B, $t = 0$–4 h), the fraction of left-migrating ECs increased significantly, and the fraction of right-migrating cells decreased significantly, indicating that ECs migrated preferentially in the upstream direction during the interval. Interestingly, the

fraction of vertically migrating cells also decreased during the interval, suggesting that a subpopulation of these cells were reorienting to migrate in the upstream direction. During the interval 4–8 h after onset of shear stress, the fractions of left- and right-migrating cells recovered to a random distribution, while the fraction of vertically migrating cells remained slightly reduced. After 8 h of shear stress, the fraction of vertically migrating cells became elevated, suggesting that most of the cells that were previously vertically migrating were now right-migrating. Finally, during the interval 12–16 h after onset of shear stress, the fraction of right-migrating cells increased, and the fraction of left-migrating cells decreased. The redistribution of migration directions indicated that that ECs were migrating preferentially in the downstream direction during the interval. Since the preferential migration direction after onset of shear stress was first upstream, then nearly random, and finally downstream, ECs in unpatterned confluent monolayers exhibited a triphasic mechanotaxis behavior as described previously.[25]

Since ECs in the center zones of 100–200-μm wide micropatterned lines exhibited polygonal morphology similar to that in unpatterned confluent monolayers, migration directions of cells in center zones of horizontal or vertical lines (Figure 1A) were estimated in order to determine whether they responded to shear stress in a manner similar to that of polygonal ECs in an unpatterned confluent monolayer. Before onset of shear stress (Figure 3C, $t < 0$ h), the fractions of left-, right-, and vertically migrating cells in center zones of horizontal lines were not significantly different from their expected values (average of 411 cells tracked per 20-min interval), indicating that migration directions were random. After onset of shear stress parallel to the horizontal lines (left-to-right), the fraction of left-migrating cells transiently increased and the fractions of right- and vertically migrating cells decreased during the first 4-h interval (Figure 3C, $t > 0$ h). This behavior was similar to that of polygonal ECs in unpatterned confluent monolayers. Interestingly, the fraction of left-migrating cells remained somewhat elevated until 8 h after onset of shear stress, at which time the distribution shifted to become mostly right-migrating. Overall, ECs in center zones of horizontal lines exhibited a triphasic mechanotaxis response similar to that of ECs in unpatterned confluent monolayers.

In order to determine whether the orientation of the micropatterned lines contributed to the triphasic mechanotaxis, ECs in center zones of vertical lines were examined (Figure 1A). Before onset of shear stress (Figure 3D, $t < 0$ h), migration directions were random (average of 123 cells tracked per 20-min interval). After onset of shear stress ($t > 0$ h), a transient increase in left-migrating cells during the first 4-h interval did not occur. Interestingly, during the interval 12–16 h after onset of shear stress, the fraction of vertically migrating cells increased, and the fraction of left-migrating cells decreased. These results suggest that ECs were migrating preferentially in the directions of the micropatterned line (vertically) but with a bias towards the downstream edge. Such behavior is consistent with physical limitation of available adhesion area of the final phase of the triphasic mechanotaxis response.

Shear Stress–Induced Migration of ECs in Quasi-Confluent Layers When Cell Shape Is Elongated

ECs migrating on narrower micropatterned lines may not respond to shear stress simply because of a limitation in available adhesion area, whereas elongated ECs located in the edge zones of wider micropatterned lines may be capable of changing migration direction towards the center of the lines. If migration direction in the half-plane bounded by the micropattern edge were random, then the expected fraction of vertically migrating cells would be 0.5 since the compartment boundary from 45° to 135° occupies 50% of the unit semicircle. Similarly, the expected fractions of left- and right-migrating cells would be 0.25. As expected before onset of shear stress, the time-averaged fraction of vertically migrating

ECs in the edge zones of horizontal lines was 0.16±0.03, and the sum of fractions of left- and right-migrating cells combined was 0.84±0.03 (Figure 4A, $t < 0$ h). Thus, cell migration direction in the edge zone was oriented primarily along the line axis. After onset of shear stress, the fractions of left-, right-and vertically migrating edge cells did not change significantly, although increased fluctuation in the values was observed. Importantly, the fraction of left-migrating cells was not significantly different from the fraction of right-migrating cells during all intervals before and after onset of shear stress. Thus, elongated ECs in edge zones of horizontal lines migrated along the line axis equally in both directions, and a triphasic mechanotaxis effect after onset of shear stress was not apparent.

In the middle zones, defined to be between the edge zones and the center zone of each micropatterned line (Figure 2A), and intermediate degree of cell shape elongation existed, suggesting the hypothesis that these ECs would exhibit intermediate mechanoresponsiveness. Before onset of shear stress, the time-averaged fraction of vertically migrating cells in the middle zones of horizontal lines was 0.35±0.05 (Figure 4B), which was less than that in the center zone and greater than that in the edge zones. In addition, the fractions of left- and right-migrating cells were less than those of cells in the edge zones. Thus, the distribution migration directions in the middle zones in the absence of shear stress was preferentially parallel to the line axis, but the influence of the pattern geometry was less than that on cells located in the edge zones. During the first 4-h interval after onset of shear stress oriented from left to right, the fraction of left-migrating cells increased transiently at the same time as a decreased in the fraction of right-migrating cells, indicating that ECs migrated preferentially in the upstream direction during the interval. During the next 4-h interval (4–8 h), the fractions of left- and right-migrating cells returned to baseline values. Beginning at 8 h after onset of shear stress, the fraction of right-migrating cells increased gradually as cell migration direction became reoriented parallel to the shear stress direction, and the fractions of left-migrating and vertically migrating cells decreased. Thus, even though ECs located in the middle zones of horizontal lines were influenced by the pattern geometry before onset of shear stress, they exhibited triphasic mechanotaxis behavior after onset of shear stress that was similar to the triphasic mechanotaxis of cells in the center zones and in unpatterned monolayers.

Although ECs in edge zones of horizontal lines did not exhibit triphasic mechanotaxis, it was possible that a change in migration of those cells was not apparent because they were already migrating parallel to the shear stress axis. Thus, elongated ECs in the edge zones of vertical lines were examined. Downstream migration of ECs along the upstream edge of the patterns or upstream migration of ECs along the downstream edge of the patterns would indicate that the cells were capable of mechanotaxis and that the physical limitation of adhesion area was inhibiting a complete mechanotaxis response. However, ECs located in the edge zones of vertical lines (Figure 4C–D) exhibited behavior similar to those located in edge zones of horizontal lines; the distribution of migration directions did not change significantly after onset of shear stress. In both the left edge zone (Figure 4C) and right edge zone (Figure 4D) of vertical lines, the fraction of vertically migrating cells was approx. 80% before and after onset of shear stress, even though adhesive areas were available towards the center of the patterns. In the left edge zone (Figure 4C), more cells were right-migrating than left-migrating, and in the right edge zone (Figure 4D), more cells were left-migrating than right-migrating. Since the proportions of left- and right-migrating cells were unchanged after onset of shear stress, these differences in direction reflected the influence of the boundary of available adhesion area that was established by the micropattern. Overall, initially elongated cells in the edge zones of vertical lines did not undergo mechanotaxis.

ECs located in the left middle zone (Figure 4E) and right middle zone (Figure 4F) of vertical lines exhibited migration behavior that was slightly biased towards the vertical direction.

The fractions of right- left- and vertically migrating cells did not change after onset of shear stress. Taken together, these data indicate that the migration directions of ECs located in the middle zones of vertical wide lines were somewhat biased by the pattern geometry and were not influenced by the onset of shear stress.

Shear Stress–Induced Migration of ECs in Quasi-Confluent Layers When Cell Shape Is Initially Elongated and then Released

Micropatterned lines demonstrated that the ability of ECs to undergo mechanotaxis in a quasi-confluent layer varied with the pre-existing cell shape. In order to test the idea that releasing geometric restriction on cell shape enables responsiveness of migration behavior to onset of shear stress, scratch wounds were made perpendicular to horizontal lines, thereby allowing ECs to adapt from elongated to polygonal cell shape as they began to migrate into the wound region.

ECs initially located in the edge zones of the lines exhibited pre-existing elongated shapes, with shape index 0.32±0.07. When these ECs reached the scratch boundary, they began to extend lamellipodia into the denuded area, and they gradually changed shape as the elongated structure was released. After onset of steady unidirectional shear stress in the left-to-right direction, i.e. parallel to the lines and perpendicular to the wound, the shape index of edge zone ECs located both downstream and upstream of the scratch boundary gradually increased (Figure 5B, D). The shape index of ECs located at the upstream (left) edge of the scratch wound was significantly increased 100 min after onset of shear stress, and the migration direction remained rightward (mean angle 0°) until 300 min after shear stress onset (Figure 5C). ECs located at the downstream (right) side of the scratch responded to onset of shear stress more quickly. Shape index was significantly increased after 60 min, and the migration direction was leftward (mean angle 180°) until 160 min after onset of shear stress (Figure 5E). Thus, initially elongated ECs at the upstream edge of the scratch maintained directional polarity longer than those at the downstream edge. Furthermore, cell shape change occurred before modification of directional migration under unidirectional steady shear stress.

Additional evidence for the process of cell shape release was provided by occasional experiments in which the tri(ethylene glycol)–terminated blocking reagent began failing to prevent protein and cell adhesion off the micropattern during perfusion of serum proteins. ECs in the edge zones of vertical lines, which were initially elongated along the edge and perpendicular to the direction of shear stress, first changed to a more polygonal shape and then migrated off the micropattern. When the cell shape changed from elongated to rounded or polygonal, the fraction of off-pattern ECs migrating away from the downstream edge of the pattern was significantly greater than 0.5, and the average distance that ECs traveled off-pattern was greater in the downstream than in the upstream direction (Figure 6). Thus, ECs were capable of a directional mechanotaxis response, and cell shape elongation perpendicular to the direction of shear stress slowed the response.

Shear Stress–Induced Migration of Initially Elongated ECs With Limited Cell-Cell Interactions

Either physical contact with adjacent cells or formation of intercellular junctions may influence EC migration under shear stress. For example, it was possible in quasi-confluent micropatterned layers that downstream migration in response to unidirectional shear stress was delayed by physical limits set by adjacent cells rather than due to some intrinsic cellular mechanosensing mechanism associated with cell shape elongation. In order to determine whether this could be the case, very low densities of ECs on vertical micropatterned lines were examined. ECs located at the edges of the lines were elongated along the micropattern

boundary, and ECs near the center of the lines exhibited more irregular shapes that were consistent with those of sparsely populated ECs on unpatterned substrates. In response to onset of unidirectional steady shear stress, the fraction of ECs in the center zones that were migrating in the downstream direction increased significantly, consistent with a unidirectional mechanotaxis response.

In the edge zones of the vertical micropatterns, elongated single/subconfluent ECs migrated primarily along the elongation axis, even though adhesion area was available towards the center of the micropatterns. ECs initially located in the left (upstream) and right (downstream) edge zones were analyzed separately after onset of shear stress in the left-to-right direction (Figure 7). Before onset of shear stress, 75–80% of cells in both the left and right edge zones were migrating vertically, i.e. parallel to the pattern edge. In the left edge zone, the fraction of vertically migrating cells decreased, and the fraction of right-migrating cells increased after onset of shear stress (Figure 7A). After 16 h of shear stress, the fractions of vertically and right-migrating cells each reached approx. 0.5. In contrast, in the right edge zone, the fraction of vertically migrating cells did not change significantly for 16 h after onset of shear stress, remaining at a level of 0.7–0.8 (Figure 7B). Thus, initially elongated cells near the downstream edge of the micropattern continued to migrate vertically rather than adapt to shear stress.

Analysis of EC shape and migration direction in the edge zones was performed in order to measure the timing of mechanotaxis behavior. Initially elongated ECs located in the left (upstream) edge zone were observed to extend protrusions in the downstream direction after onset of unidirectional steady shear stress. During this process, ECs became less elongated and gradually turned away from the vertical orientation. Consistent with these observations, the shape index of these cells gradually increased after onset of shear stress and became significantly greater than the no-flow value after 2 h (Figure 8A). The mean migration angle of ECs in the left edge zone was bimodal and clustered around 90° before onset of shear stress, consistent with equal numbers of cells migrating in both directions along the vertical axis (Figure 8B). The distribution of migration angles remained primarily bimodal until 7 h after onset of shear stress. At this time, the distribution changed rapidly to a unimodal cluster around 0°, i.e. in the direction of shear stress. In contrast, the mean migration angle of ECs in the right edge zone remained primarily bimodal and clustered around 90° even after 16 h of shear stress (Figure 8C), indicating that equal numbers of cells continued to migrate in both directions along the vertical axis parallel to the micropattern edge. These data demonstrate that a time lag of order 6 h exists between cell shape change and reorientation of migration direction, which is consistent with cytoskeletal and shape reorganization time scales of adaptation to shear stress.

DISCUSSION

ECs in a confluent monolayer exhibit polygonal cell shape and structure, with randomly oriented stress fibers and focal adhesions. After onset of steady unidirectional shear stress, these ECs develop a triphasic mechanotaxis behavior that consists of migration first in the upstream direction, then in more heterogeneous directions, and finally in the downstream direction.[25] In contrast, ECs on micropatterned lines with elongated shape and structure lost coordinated directional migration after onset of shear stress. Here, micropatterned lines of width 100–200 μm were implemented to create monolayers of ECs with gradually varying shapes. This strategy enabled two major advances: (1) migration behavior of ECs with different geometric limitations could be investigated simultaneously, and (2) elongated ECs located near the upstream edge of a line oriented perpendicular to the shear stress direction could theoretically migrate in the downstream direction.

We previously reported that 20-μm micropatterned lines preset ECs to an elongated and aligned structure[25] with shape index that was similar ECs after adaptation to steady unidirectional shear stress.[27] These elongated cells did not respond to onset of shear stress by exhibiting a triphasic mechanotaxis behavior but instead lost coordinated directional migration characteristics, independently of whether shear stress was oriented parallel or perpendicular to the major axis of cell shape. However, the geometric limitation imposed by the micropattern boundary also limited the available area of extracellular matrix protein to support cell migration; therefore, migration speed in the direction of the micropatterned strip was expected to be increased.[23] ECs located at the edges of wider 100–200-μm patterns exhibited a similar shape index value, but the pattern width did not restrict the ability of ECs to change shape or migration direction in response to onset of shear stress. Nevertheless, ECs continued to migrate primarily along the micropattern edge even in the presence of shear stress. Furthermore, the direction of shear stress with respect to the micropatterned line axis did not alter migration in the edge zones of the micropatterned lines. These results suggest that EC shape and structure controlled migration under shear stress rather than the micropattern width per se.

A second possibility for control of EC mechanotaxis in a quasi-confluent monolayer is a mechanism based on physical or chemical communication with adjacent cells. Indeed, the triphasic mechanotaxis behavior of ECs in a confluent monolayer is distinct from the immediately directional mechanotaxis of isolated ECs on an unpatterned substrate.[24, 25] Intercellular communication among adjacent ECs after onset of shear stress occurs biochemically through mechanisms that include gap junction–mediated signaling[8] and release of paracrine factors.[10, 16] In addition, cell-modulated physical cues in the microenvironment such as rapid remodeling of the extracellular matrix[15, 26, 33] or adherens junctions[28, 35] may mediate mechanotransmission of forces among cells, thereby regulating force-dependent generation of traction forces involved in cell migration. Despite the existence of these mechanisms, ECs in a confluent monolayer are capable of migrating along mutually independent paths in spite of physical boundaries established by adjacent cells, as demonstrated by random walk models fitted to migration trajectories.[31] In addition, ECs located in the upstream edge zone of wider lines did not migrate immediately in the direction of shear stress, even in the absence of adjacent cells. Finally, comparison of total immunolabeled fibronectin to micropatterned fluorescent fibronectin suggested that most cell-derived fibronectin remained intracellular, and extracellular fibronectin was not significantly remodeled during the experiments. These observations suggest that cell-cell contact and extracellular matrix remodeling were not dominant factors in limiting the mechanotaxis behavior of elongated ECs.

Although presetting ECs into an elongated structure suppressed mechanotaxis behavior under flow, these cells were able to resume the responsiveness to flow once the preset elongated structure was released. When a scratch wound was made perpendicular to the micropatterned lines or when the surface blocking reagent was compromised, ECs first remodeled their shape to one that was less elongated and then began to migrate preferentially in the direction of shear stress. The time delay between shape change and onset of directional migration suggests that constant maintenance of cell elongation was required to suppress mechanotaxis. Further evidence for this idea was observed in the behavior of isolated ECs on the wide patterns oriented perpendicular to the shear stress direction. Cells in the center regions of wide micropatterns showed immediate downstream mechanotaxis, similar to single cells on unpatterned substrates. Cells in the right edge zones continued to migrate along their elongation axis, since their elongated shapes were maintained by the micropattern edge. However, single elongated cells in the edge zones of wide vertical patterns continued to migrate along their elongation direction after onset of perpendicular flow until their preset elongated shape was released. Only after 7 h of

perpendicular flow did cells in the left edge zone show downstream mechanotaxis. What caused these cells to suddenly change shape and migrate in the downstream direction remains unknown.

How did controlling cell structure determine migration behavior under shear stress? When cells took an elongated shape on narrow micropatterns or at the edges of wider patterns, actin stress fibers and focal adhesion sites were orientated preferentially along the major axis.[23, 25] Valid hypotheses are that intracellular prestress was oriented along the cell elongation axis, and the traction forces were generated mainly at the ends of the cells, as measured in fibroblasts grown on high–aspect ratio rectangular islands.[11] Since traction force directly dictates cell migration direction, elongated cells were expected to migrate preferentially along the structural elongation axis in the absence of shear stress. The small GTPase RhoA has been implicated in the process of shear-mediated EC motility on unpatterned surfaces.[30] A transient peak in RhoA-GTP levels at 30 min after onset of steady unidirectional shear stress correlates with both cell speed and mean traction force in isolated, polarized ECs on a fibronectin substrate. Importantly, the spatial locations of maximum traction force magnitude correspond to sites of uropod or lamellipod detachment and to sites adjacent to the advancing lamella front. One might predict that a similar distribution of traction forces at the ends of ECs elongated on narrow micropatterned lines would contribute to increased migration speed in the absence of shear stress.[25] However, since directional mechanotaxis and increased migration speed did not occur in ECs on narrow lines, mechanoregulation of this pathway in elongated cells must be more complex. Although traction forces have not yet been measured in micropatterned ECs during exposure to shear stress, RhoA activity is required for shear-mediated cell survival and actin stress fiber reinforcement to occur on an adaptation time scale.[37] Taken together, these ideas imply that the initial RhoA activation in isolated, unpatterned ECs in response to onset of shear stress serves to redistribute intracellular prestress and traction force to support mechanotaxis. In micropatterned, elongated ECs, this process is likely to be frustrated by the inability to establish new cell-matrix adhesion sites in areas off the micropattern, leading to decreased migration speed and a significant time delay (several hours) before adaptive reinforcement of cytoskeletal structure begins to alter the axial distribution of intracellular prestress after onset of shear stress. Release of structural elongation and onset of shape adaptation mediated by new integrin ligation and adhesion formation[34] would result in a more spatially heterogeneous distribution of intracellular cytoskeletal tension and traction force generation, which would enable mechanotaxis to occur. In order to test this model, the spatial distribution of RhoA activity and traction force generation in ECs within confluent monolayers (patterned and unpatterned) will be required.

In general, the inhibition of mechanotaxis in elongated ECs supports the idea that adaptation to anti-atherogenic flow profiles serves to desensitize mechanotransduction pathways in endothelium.[29] In most cell culture models of mechanotransduction, onset of steady unidirectional shear stress serves as a large environmental change that promotes rapid disassembly and reorganization of the cytoskeleton. However, ECs in vivo generally experience only small or gradual perturbations of shear stress, and cytoskeletal structure and cell shapes that are already adapted to the local hemodynamic profile may be less responsive to those perturbations. For example, in atherosclerosis-resistant regions of the artery wall, an elongated cell shape and well-organized stress fiber network may confer lower mechanosensitivity to physiological changes in hemodynamic forces that occur with normal physiological activity. Thus, in vitro models using micropatterning have been developed to elucidate mechanotransduction mechanisms in ECs that are preconditioned to a physiological shear stress profile.[2, 13] In the present studies, micropatterned substrates served to preset ECs into a morphology that mimics that of ECs in atherosclerosis-resistant artery walls. For the first time, these experiments demonstrate that mechanotaxis after onset

of unidirectional shear stress required dynamic reorganization of cell shape before migration direction could be altered. Thus, mechano-adaptation of cytoskeletal structure and cell shape modifies the endothelial response to perturbations in shear stress profile.

Acknowledgments

This study was supported by NIH grants HL-071958 and HL-080956.

ABBREVIATIONS

EC	endothelial cell
PEG	poly(ethylene glycol)

References

1. Abramoff MD, Magelhaes PJ, Ram SJ. Image processing with ImageJ. Biophotonics Intl. 2004; 11:36–42.
2. Blackman BR, Garcia-Cardena G, Gimbrone MA Jr. A new in vitro model to evaluate differential responses of endothelial cells to simulated arterial shear stress waveforms. J Biomech Eng. 2002; 124:397–407. [PubMed: 12188206]
3. Brock A, Chang E, Ho CC, Leduc P, Jiang X, Whitesides GM, Ingber DE. Geometric determinants of directional cell motility revealed using microcontact printing. Langmuir. 2003; 19:1611–1617. [PubMed: 14674434]
4. Choi CK, Helmke BP. Short-term shear stress induces rapid actin dynamics in living endothelial cells. Mol Cell Biomech. 2009 in press.
5. Coomber BL, Gotlieb AI. In vitro endothelial wound repair. Interaction of cell migration and proliferation. Arteriosclerosis. 1990; 10:215–222. [PubMed: 1969263]
6. Cunningham KS, Gotlieb AI. The role of shear stress in the pathogenesis of atherosclerosis. Lab Invest. 2004; 85:9–23. [PubMed: 15568038]
7. Davies PF, Polacek DC, Handen JS, Helmke BP, Depaola N. A spatial approach to transcriptional profiling: mechanotransduction and the focal origin of atherosclerosis. Trends Biotechnol. 1999; 17:347–351. [PubMed: 10461179]
8. Depaola N, Davies PF, Pritchard WF Jr, Florez L, Harbeck N, Polacek DC. Spatial and temporal regulation of gap junction connexin43 in vascular endothelial cells exposed to controlled disturbed flows in vitro. Proc Natl Acad Sci USA. 1999; 96:3154–3159. [PubMed: 10077653]
9. Dewey CF Jr, Bussolari SR, Gimbrone MA Jr, Davies PF. The dynamic response of vascular endothelial cells to fluid shear stress. J Biomech Eng. 1981; 103:177–188. [PubMed: 7278196]
10. Dull RO, Davies PF. Flow modulation of agonist (ATP)-response (Ca^{2+}) coupling in vascular endothelial cells. Am J Physiol. 1991; 261:H149–154. [PubMed: 1858915]
11. Li, Fang; BLQ-M; WJHCW. Cell shape regulates collagen type I expression in human tendon fibroblasts. Cell Motility and the Cytoskeleton. 2008; 65:332–341. [PubMed: 18240273]
12. Fisher, NI. Statistical analysis of circular data. Cambridge: Cambridge University Press; 1993.
13. Gelfand BD, Epstein FH, Blackman BR. Spatial and spectral heterogeneity of time-varying shear stress profiles in the carotid bifurcation by phase-contrast MRI. J Magn Reson Imaging. 2006; 24:1386–1392. [PubMed: 17083089]
14. Gimbrone MA, Resnick N, Nagel T, Khachigian LM, Collins T, Topper JN. Hemodynamics, endothelial gene expression, and atherogenesis. Ann NY Acad Sci. 1997; 811:1–10. [PubMed: 9186579]
15. Gupte A, Frangos JA. Effects of flow on the synthesis and release of fibronectin by endothelial cells. In Vitro Cell Dev Biol. 1990; 26:57–60. [PubMed: 2407710]
16. Hecker M, Mulsch A, Bassenge E, Busse R. Vasoconstriction and increased flow: two principal mechanisms of shear stress-dependent endothelial autacoid release. Am J Physiol. 1993; 265:H828–833. [PubMed: 8105699]

17. Helmke BP, Goldman RD, Davies PF. Rapid displacement of vimentin intermediate filaments in living endothelial cells exposed to flow. Circ Res. 2000; 86:745–752. [PubMed: 10764407]
18. Hsu PP, Li S, Li YS, Usami S, Ratcliffe A, Wang X, Chien S. Effects of flow patterns on endothelial cell migration into a zone of mechanical denudation. Biochem Biophys Res Comm. 2001; 285:751–759. [PubMed: 11453657]
19. Hsu S, Thakar R, Liepmann D, Li S. Effects of shear stress on endothelial cell haptotaxis on micropatterned surfaces. Biochem Biophys Res Comm. 2005; 337:401–409. [PubMed: 16188239]
20. Jiang X, Bruzewicz DA, Wong AP, Piel M, Whitesides GM. Directing cell migration with asymmetric micropatterns. Proc Natl Acad Sci USA. 2005; 102:975–978. [PubMed: 15653772]
21. Lamalice L, Le Boeuf F, Huot J. Endothelial cell migration during angiogenesis. Circ Res. 2007; 100:782–794. [PubMed: 17395884]
22. Levesque MJ, Nerem RM. The elongation and orientation of cultured endothelial cells in response to shear stress. J Biomech Eng. 1985; 107:341–347. [PubMed: 4079361]
23. Li S, Bhatia S, Hu YL, Shiu YT, Li YS, Usami S, Chien S. Effects of morphological patterning on endothelial cell migration. Biorheology. 2001; 38:101–108. [PubMed: 11381168]
24. Li S, Butler PJ, Wang Y, Hu Y, Han DC, Usami S, Guan JL, Chien S. The role of the dynamics of focal adhesion kinase in the mechanotaxis of endothelial cells. Proc Natl Acad Sci USA. 2002; 99:3546–3551. [PubMed: 11891289]
25. Lin X, Helmke BP. Micropatterned structural control suppresses mechanotaxis of endothelial cells. Biophys J. 2008; 95:3066–3078. [PubMed: 18586851]
26. Mott RE, Helmke BP. Mapping the dynamics of shear stress-induced structural changes in endothelial cells. Am J Physiol. 2007; 293:C1616–C1626.
27. Nerem RM, Levesque MJ, Cornhill JF. Vascular endothelial morphology as an indicator of the pattern of blood flow. J Biomech Eng. 1981; 103:172–177. [PubMed: 7278195]
28. Noria S, Cowan DB, Gotlieb AI, Langille BL. Transient and steady-state effects of shear stress on endothelial cell adherens junctions. Circ Res. 1999; 85:504–514. [PubMed: 10488053]
29. Robling AG, Burr DB, Turner CH. Recovery periods restore mechanosensitivity to dynamically loaded bone. Journal of Experimental Biology. 2001; 204:3389–3399. [PubMed: 11606612]
30. Shiu YT, Li S, Marganski WA, Usami S, Schwartz MA, Wang YL, Dembo M, Chien S. Rho mediates the shear-enhancement of endothelial cell migration and traction force generation. Biophys J. 2004; 86:2558–2565. [PubMed: 15041692]
31. Simmers MB, Pryor AW, Blackman BR. Arterial shear stress regulates endothelial cell-directed migration, polarity, and morphology in confluent monolayers. Am J Physiol. 2007; 293:H1937–1946.
32. Sprague EA, Luo J, Palmaz JC. Human aortic endothelial cell migration onto stent surfaces under static and flow conditions. J Vasc Interv Radiol. 1997; 8:83–92. [PubMed: 9025045]
33. Thoumine O, Nerem RM, Girard PR. Changes in organization and composition of the extracellular matrix underlying cultured endothelial cells exposed to laminar steady shear stress. Lab Invest. 1995; 73:565–576. [PubMed: 7474929]
34. Tzima E, Del Pozo MA, Shattil SJ, Chien S, Schwartz MA. Activation of integrins in endothelial cells by fluid shear stress mediates Rho-dependent cytoskeletal alignment. EMBO J. 2001; 20:4639–4647. [PubMed: 11532928]
35. Ukropec JA, Hollinger MK, Woolkalis MJ. Regulation of VE-cadherin linkage to the cytoskeleton in endothelial cells exposed to fluid shear stress. Exp Cell Res. 2002; 273:240–247. [PubMed: 11822879]
36. Wootton DM, Ku DN. Fluid mechanics of vascular systems, diseases, and thrombosis. Annu Rev Biomed Eng. 1999; 1:299–329. [PubMed: 11701491]
37. Wu CC, Li YS, Haga JH, Kaunas R, Chiu JJ, Su FC, Usami S, Chien S. Directional shear flow and Rho activation prevent the endothelial cell apoptosis induced by micropatterned anisotropic geometry. Proc Natl Acad Sci USA. 2007; 104:1254–1259. [PubMed: 17229844]

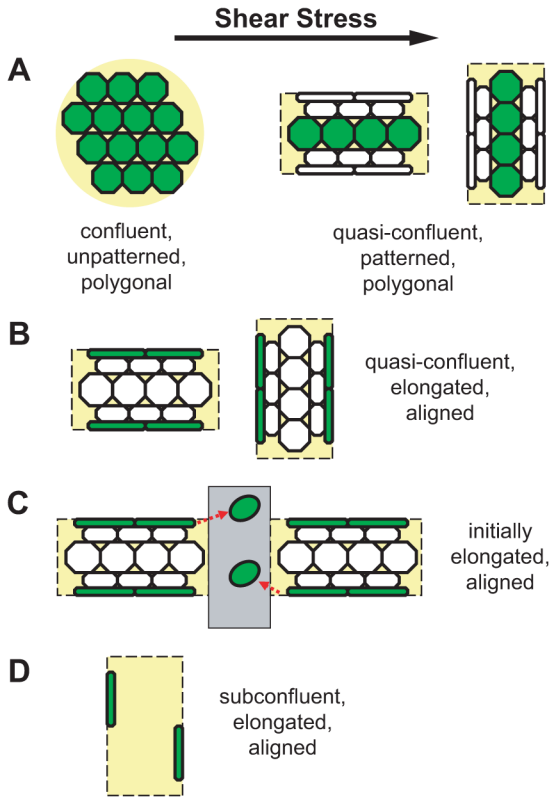

Figure 1.
Schematic of experimental strategy using micropatterning. Cells of interest are green, and shear stress direction is left-to-right. (A) Polygonal ECs in a confluent monolayer or in a quasi-confluent state in the center zones of wide micropatterned lines. Adhesion area is available in all directions. (B) Elongated, aligned ECs in the edge zones of wide lines. Adhesion area is available towards the center zones. (C) Initially elongated, aligned ECs migrating from the edge zones of wide lines into perpendicular scratch wounds. (D) Sparsely populated elongated, aligned ECs in the edge zones of vertical wide lines. Cells at the left edge have adhesion area available in the downstream direction, and cells at the right edge have adhesion area available in the upstream direction.

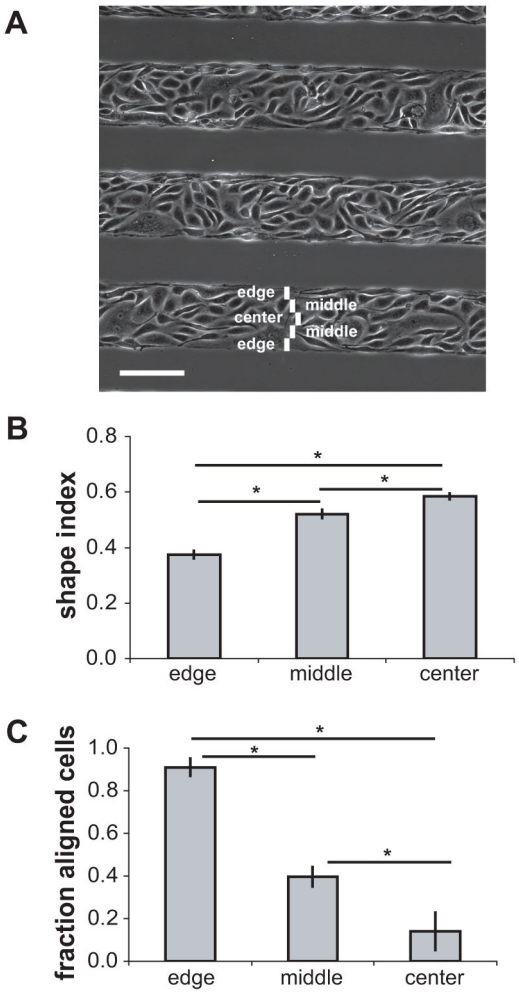

Figure 2.

Gradient of cell morphology in ECs on wide micropatterns. (A) Phase-contrast image of ECs on micropatterned lines of width 110 μm. Edge, middle, and center zones are illustrated. Scale bar, 100 μm. (B) Shape index of ECs in the edge, middle, and center zones of wide lines (error bars, SE; n=5 micropatterns; *p<0.05). (C) Fraction of aligned cells in each zone (error bars, SE; n=3 micropatterns; *p<0.05).

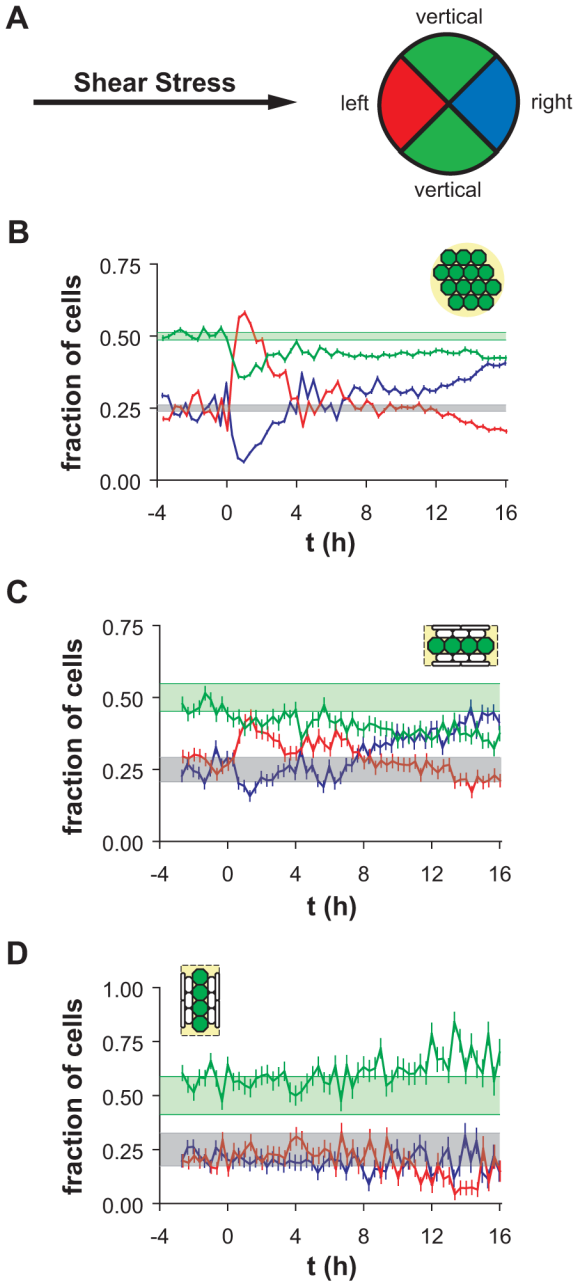

Figure 3.

Distribution of migration directions of polygonally shaped ECs before (t < 0 h) and after (t > 0 h) onset of steady unidirectional shear stress. (A) Cells were categorized as left-migrating (red), right-migrating (blue), or vertically migrating (green) with respect to the shear stress direction, left-to-right. (B) Fractions of left- (red), right-(blue), and vertically (green) migrating cells on unpatterned surfaces. Error bars, SE_p (see Methods for explanation). Shaded bands indicate 95% confidence intervals for the expected values of left- or right-migrating (gray) and vertically migrating (green) cells, computed using $\langle N \rangle = 5370$ cells tracked per 20-min interval. (C) Fractions of left- (red), right- (blue), and vertically (green) migrating cells in center zones of horizontal wider lines. Error bars, SE_p. Shaded bands indicate 95% confidence intervals for the expected values of left- or right-migrating (gray)

and vertically migrating (green) cells, computed using $<N>$ = 411 cells tracked per 20-min interval. (D) Fraction of left- (red), right- (blue), and vertically (green) migrating cells in center zones of vertical wider lines. Error bars, SE_p. Shaded bands indicate 95% confidence intervals for the expected values of left- or right-migrating (gray) and vertically migrating (green) cells, computed using $<N>$ = 123 cells tracked per 20-min interval.

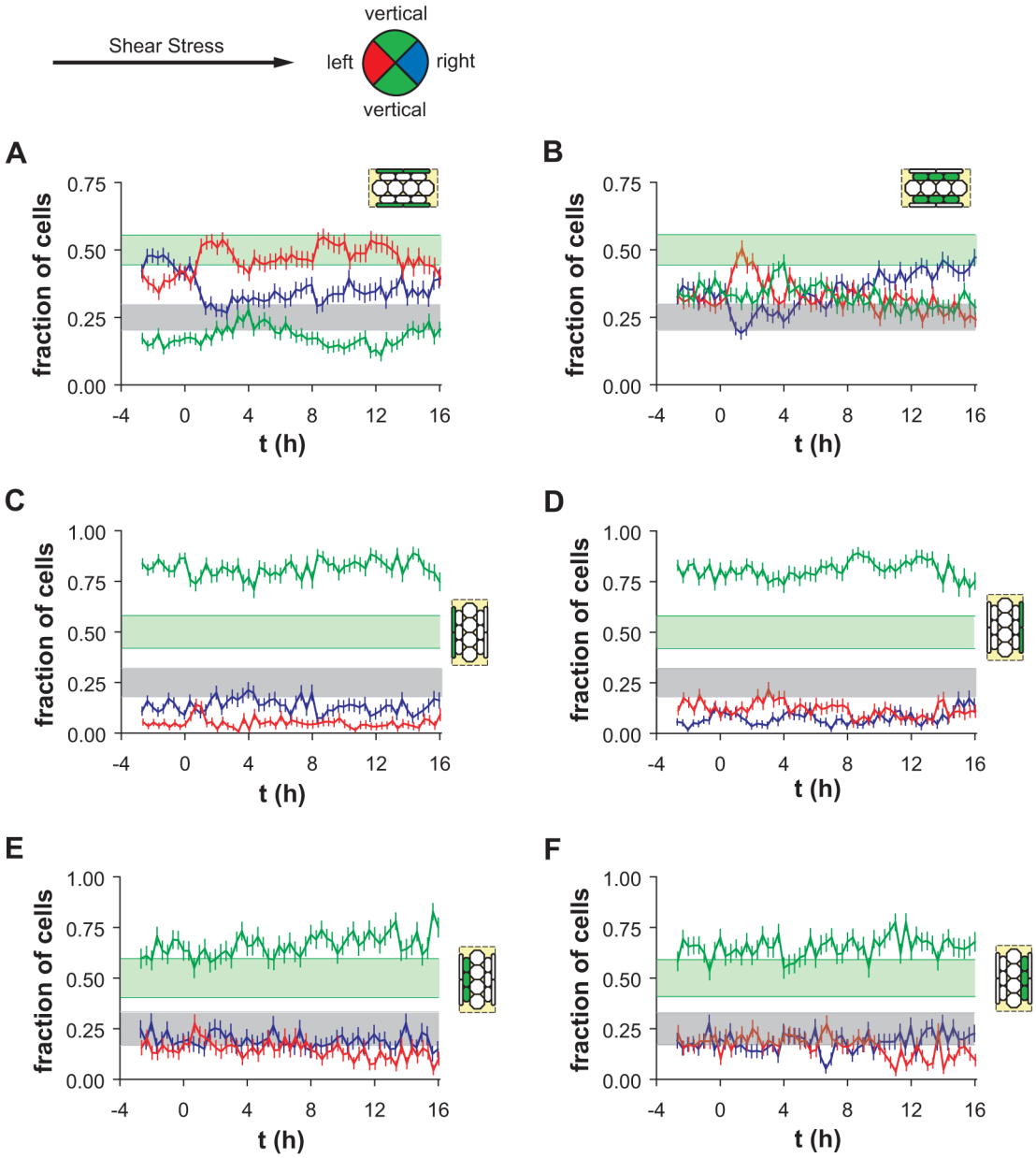

Figure 4.

Distribution of migration directions before and after onset of steady unidirectional shear stress for ECs (A–B) on horizontal wide patterns (A) in the edge zone (<*N*> = 318 cells) and (B) in the middle zone (<*N*> = 302 cells). (C–F) Fraction of cells migrating in each direction category for ECs on vertical wide patterns, as indicated by the schematic diagrams. (C) Left (upstream) edge zone (<*N*> = 146 cells). (D) Right (downstream) edge zone (<*N*> = 152 cells). (E) Left middle zone (<*N*> = 104 cells). (F) Right middle zone (<*N*> = 116 cells). Error bars, SE_p. Shaded bands indicate 95% confidence intervals for the expected values of left- or right-migrating (gray) and vertically migrating (green) cells, computed using <*N*> cells tracked per 20-min interval.

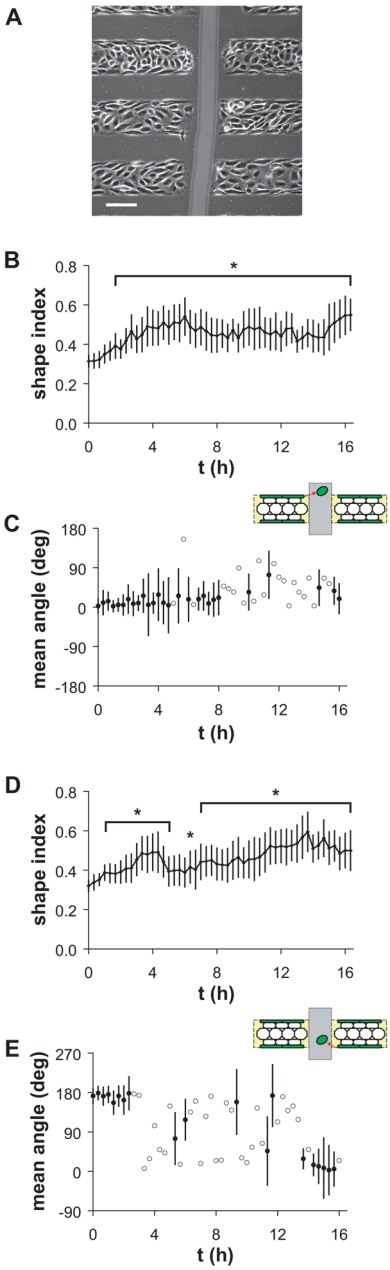

Figure 5.

Migration of elongated ECs off micropatterned lines into a scratch wound after onset of shear stress. (A) Phase-contrast image of cells before onset of shear stress. Scale bar, 100 μm. (B) Cell shape index and (C) mean angle of cell migration from the upstream edge of the vertical scratch, as indicated in the schematic. (D) Cell shape index and (E) mean angle of cell migration from the downstream edge of the vertical scratch, as indicated in the schematic. Error bars, 95% confidence intervals. *Shape index significantly different than at $t = 0$ h ($p<0.05$, t-test, $n>20$ cells). Closed circles indicate migration angles significantly clustered around the mean angle ($p<0.05$, Rayleigh test). Open circles indicate migration angles not significantly different from the uniform distribution (i.e. confidence interval includes the entire circle).

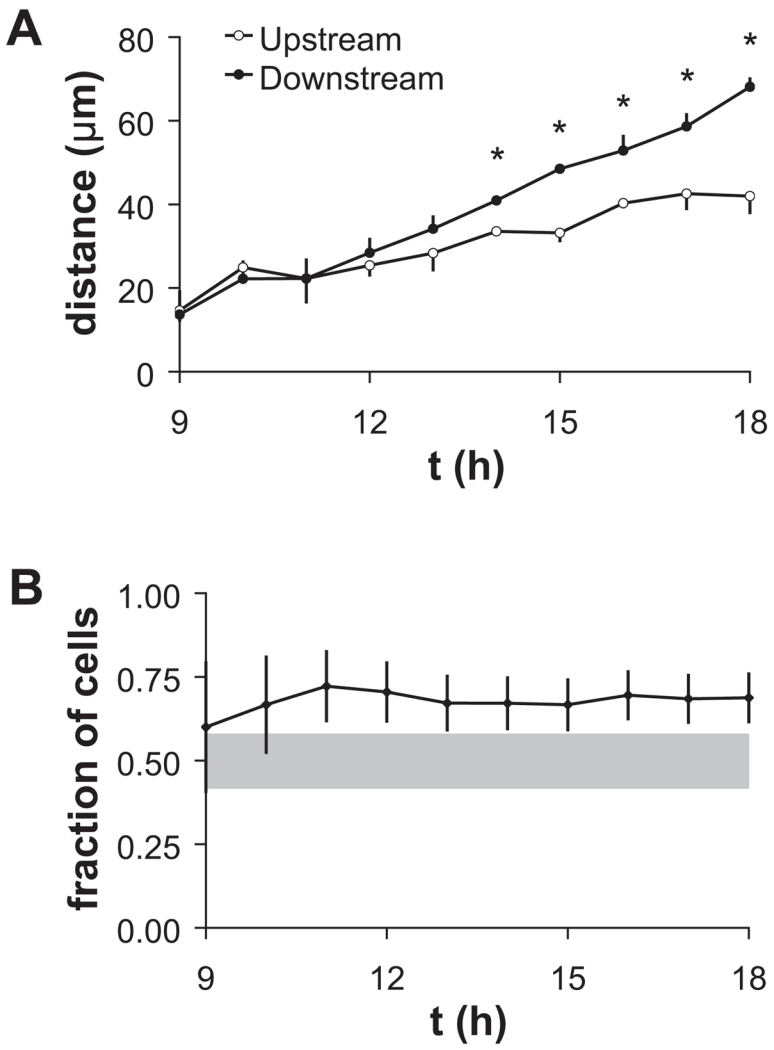

Figure 6.

Cell migration off vertical patterns after onset of shear stress when blocking reagent failed. (A) Average distance between off-pattern cell position and the edge of the pattern. Error bars, SE; n=4 fields of view. *Distance off-pattern of downstream cells was significantly larger than of upstream cells (*t*-test, $p<0.05$). (B) Fraction of cells off-pattern migrating in downstream direction. Error bars, SE_p. Shaded band indicates 95% confidence interval for the expected value if migration upstream or downstream occurred with equal probability.

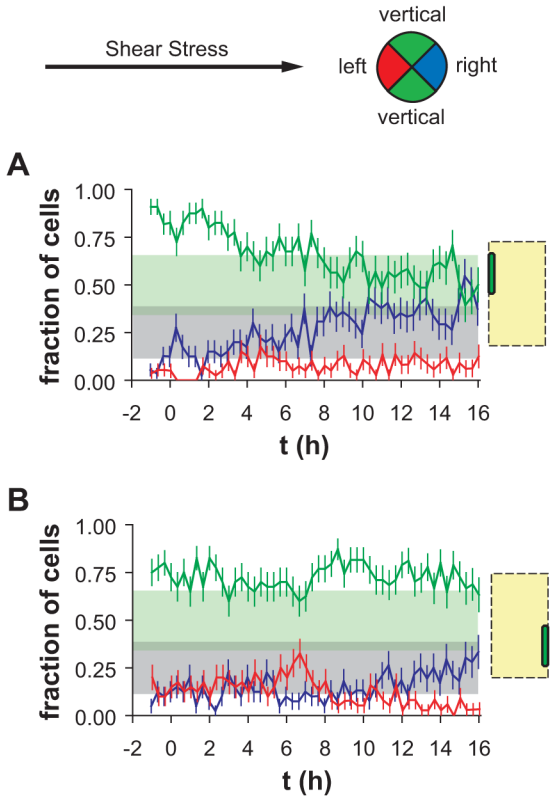

Figure 7.

Fractions of left-migrating (upstream), right-migrating (downstream), and vertically migrating single cells (A) on the left edge and (B) on the right edge of vertical wider patterns. Error bars, SE_p; $N = 40$ cells. Shaded bands indicate 95% confidence intervals for the expected values of left- or right-migrating (gray) and vertically migrating (green) cells, computed using N cells tracked per 20-min interval.

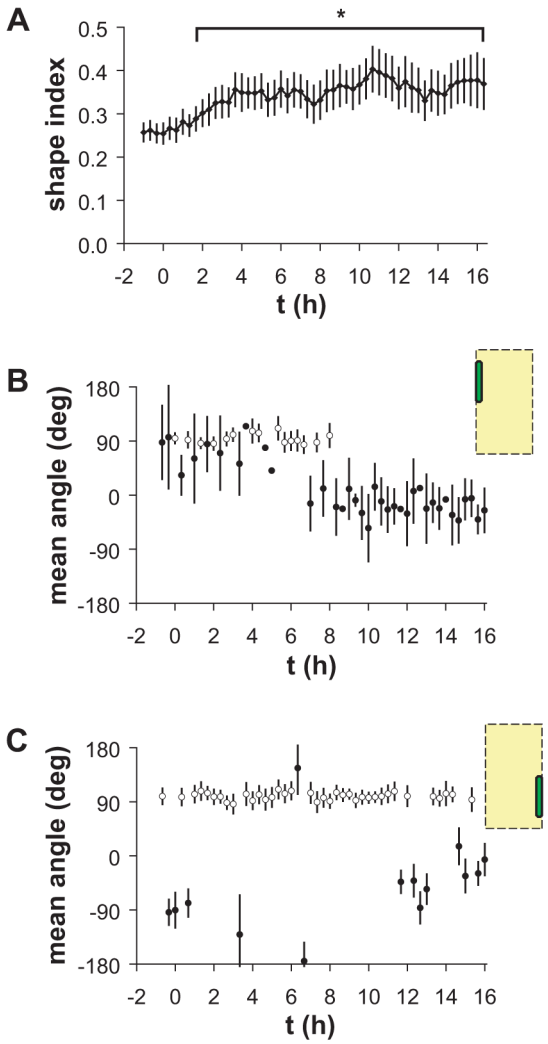

Figure 8.

Morphology and migration of isolated single ECs on vertical wide patterns. (A) Shape index of cells in the left edge zone before and after onset of shear stress oriented perpendicular to the lines. Error bars, CI; n=40 cells; *significantly greater than no-flow value (*t*-test, p<0.05). (B–C) Mean angle of migration of cells (B) in the left edge zone and (C) in the right edge zone. Error bars, 95% confidence interval; n=40 cells. Closed circles indicate unimodal migration angles significantly clustered around the mean angle (p<0.05, Rayleigh test). Open circles indicate bimodal migration angles significantly clustered around the mean axis (p<0.05, Rayleigh test).